# Ionic and Chain Interdiffusion and Interfacial Strength Development in Ionomers of Poly(ethylene-*co*-methacrylic acid)

**John G. Van Alsten**

*Central Research & Development, E. I. du Pont de Nemours & Co., Experimental Station, Wilmington, Delaware 19880-0356*

*Received March 29, 1995; Revised Manuscript Received August 8, 1995*[⊗]

ABSTRACT: Diffusion coefficients of sodium and zinc ions have been measured in bilayers of commercial, partially neutralized poly(ethylene-*co*-methacrylic acid). The diffusion behavior shows a break at the melting temperature of the resin, suggesting that chain backbone motion is intimately related to ionic transport. The ionic diffusion coefficients are orders of magnitude greater than those of the chain backbone, which suggests that metal ion pairs are transported along the contour of the polymer network via exchange with protons of neighboring acid groups. Interfacial strength development in welded films of ionomers is primarily determined by the melting behavior of the bulk resin. Ionic diffusion rates do not correlate with the strength development behavior. This observation, along with melting and chain center of mass diffusion information, suggests that strength development is dependent on chain interdiffusion like that of many other thermoplastics.

The development of mechanical strength across polymer interfaces has been the subject of intense study, driven by the great commercial importance of producing polymer laminates. It is now generally accepted that good interfacial strength necessitates some degree of intermixing of the contacting polymer phases,[1] although the absolute depth to which the interdiffusion process must proceed has been difficult to generalize, varying from a few angstroms for poly(methyl methacrylate)[2] to several hundred angstroms in some polyimides.[3] Our own interests have concentrated on interfacial development in systems where at least one of the components is phase segregated and therefore presumably unable to execute the center of mass transport required for extensive intermixing. Examples of these include bilayers of semicrystalline and compatible amorphous polymers[4,5] and those of poly(urethane urea) elastomers.[6] Despite the various degrees of restriction imposed by the chain anchoring microstructures in these examples, a very high degree of interfacial strength is still achievable.

One of the most familiar examples of polymer welding is in the packaging of foods, where the foodstuffs are first dropped into polymer bags that are subsequently sealed with a hot bar. The sealing functionality in these materials is typically provided by an appropriate copolymer of ethylene, such as ethylene-*co*-α-olefin, vinyl acetate, or acrylic or methacrylic acid. A recent series of publications[7,8] provided a very comprehensive examination relating the performance characteristics of these materials to chain microstructure. This study emphasized that the melting behavior of the resin is by far the most critical aspect in determining the ability of such resins to form good interfacial seals over the time scales of the process. Complete melting of the resin was found not to be required for the development of strength, although certainly a necessity for optimum performance.

We have been studying related but far more complicated packaging systems, namely the ionomers produced by the partial neutralization of poly(ethylene-*co*-methacrylic acid), which are marketed by DuPont under the trade name Surlyn. Ionomers are the subject of much study and a rich literature.[9−11] Briefly, the inclusion of a small fraction of highly polar ionic groups into an otherwise low dielectric constant polymer backbone results in the segregation of ionic groups into small domains, or "multiplets". These multiplets act as transient cross-links in the system and have a profound impact on the rheological behavior of the material. In one of the materials we shall discuss here, for example, neutralization of the parent acid copolymer to a total ionic content of ca. 1.5% results in an increase in melt viscosity of over 20 times. The rheological behavior of ionomers has been shown to be dependent on numerous factors, such as ion type and degree of neutralization, the stiffness of the chain backbone, and the polarity of the melt.[11]

Ionomers are also well recognized to provide superior performance in heat-sealing applications, particularly those in which surfaces might be contaminated by food greases. The precise details governing this performance are poorly understood. Of particular interest is the relative contribution of interphase ionic exchange to that of interphase chain entanglement to strength. In the former picture, the locations of the ionic multiplets merely rearrange and interfacial mass transfer is predominantly local in nature, requiring only a short-range motion of a small fraction of the chain to transport ions. The latter scheme would require full center of mass motion of the polymer chain. It is unclear if rearrangement of the ionic multiplet network alone is sufficient to provide good mechanical strength in these applications.

Another interesting question concerns the influence of morphology and composition on ionic mobility. Virtually all previous study of ionic diffusion in polymers has been concentrated in the membrane community and has focused on transport at high ionic concentrations, above the metal−insulator transition where the ionic phase becomes continuous. For example, Gronowski et al.[12] found that the conductivity of poly(methyl methacrylate-*co*-methacrylic acid) films increased 5 orders of magnitude around an acid concentration of 6.5%. Above this transition, diffusion coefficients of ca. $10^{-5}$ cm$^2$/s were measured, but no information on diffusion below the transition was reported. The only previous study of which we are aware is that of Vyprachticky et al.,[13] who compared the diffusion coefficients of protonated ammonium ions in acid containing polymethacrylates

[⊗] Abstract published in *Advance ACS Abstracts,* February 15, 1996.

0024-9297/96/2229-2163$12.00/0 

**Table 1. Characterization of Materials**

| material | mol % acid | % neutralization |
|---|---|---|
| sodium ionomer | 3.5 | 54 |
| zinc ionomer | 5.4 | 22 |
| E/MAA 1 | 5.4 | 0 |
| E/MAA 2 | 3.5 | 0 |

to that of the parent amine in nonacidic polymethacrylates. These authors concluded that in these polar systems the dissociation behavior of the base was critical in determining the rate of diffusion, with a bulky, more dissociated ammonium ion exhibiting faster diffusion than a smaller, more tightly bound ion. In addition, the activation energies for diffusion for the ions were significantly greater than those of the unprotonated bases, as might be expected from a thermally activated dissociation process. In the systems with which we are concerned, there is the additional complication of crystallinity, which might have a significant impact on ionic transport by preventing long-range mobility of the polymer backbone.

## Experimental Section

**Materials.** The polymers utilized were commercial materials comprised of unneutralized and partially neutralized poly(ethylene-*co*-methacrylic acid), which are marketed by DuPont under the trade names Nucrel and Surlyn. These are prepared via high-pressure free-radical polymerization and have number-average molecular weights of ca. 200 000 with polydispersities of ca. 8−9. Four different resins were utilized, a sodium ionomer, a zinc ionomer, and two acid copolymers of different acid concentration. Relevant characterizations of these materials are provided in Table 1.

**Seal Strength.** Mechanical measurements of seal strengths were obtained in a "T-peel" geometry on laminates of films 50 $\mu$m thick mounted on a nonextensible paper backing. The seal time was kept constant at 1.0 s, and the seal pressure was 0.27 MPa. Seal strengths are well known to be insensitive to laminating pressures in this range. Specimens were aged for 48 h prior to mechanical testing, which was conducted on a tensile tester at a speed of 50 cm/min.

**Calorimetry.** DSC measurements were obtained using a DuPont Instruments 9900. Copolymers of ethylene are well known to be subject to significant recrystallization upon extended aging,[14] so the initial crystallinity was first erased by heating to 150 °C. The sample was then quenched and subsequently rerun on the calorimeter. Due to the aging effect, the "second-cycle" melting behavior is much more relevant to correlating the peel and diffusion data presented here. The raw data were downloaded to a computer and the melting behavior quantified by integration of the melting endotherm.

**Diffusion Measurements.** Diffusion measurements were obtained using the infrared attenuated total reflectance (ATR) method. Detailed descriptions of the technique are presented in numerous other publications.[4−6,15] This technique measures diffusion from the temporal change in concentration of an infrared-active species within the detection volume of the ATR element. Typical experiments utilize polymer bilayers of infrared-distinguishable species. The measured absorbance is normalized between the initial and equilibrium values to provide a normalized mass uptake curve as a function of time. This curve can be predicted mathematically by convoluting a model of the spatial dependence of a species' concentration history, $C(x,t)$, with the detecting exponentially decaying electric field of the IR radiation:

$$\frac{A(t)}{A_\infty} = \frac{\int_0^\infty \alpha C(x,t) \exp\left(\frac{-2x}{\lambda}\right) dx}{\int_0^\infty \alpha C_\infty \exp\left(\frac{-2x}{\lambda}\right) dx} \quad (1)$$

In this expression, $x$ is the distance from the polymer/infrared crystal interface, $A$ is the measured absorbance, $\alpha$ is the characteristic oscillator strength, and $\lambda$ is the characteristic decay length[16] of the IR radiation. We have shown that these uptake measurements yield excellent descriptions of simple Fickian diffusion, but the technique is of course general to any situation in which the concentration profile can be represented mathematically.

Diffusion couple bilayers were produced by dip coating (ca. 2−10 $\mu$m) from solution one component directly onto the face of a 60° ZnS ATR crystal and placing this in contact with a melt-pressed thick film (ca. 150 $\mu$m) of the other material. In the case of the zinc ionomer, the ionomer was dip coated onto the crystal from DMPU at 80 °C and contacted with a melt-pressed film of the parent acid copolymer. In the case of the sodium ionomer, we measured the diffusion of ions from a thick film of the ionomer into a thin film of acid copolymer which had been dip coated from THF solution at 60 °C. For the ionomer samples, quantification was provided by integration of the characteristic carboxylate asymmetric stretches, which for *dry* materials are found at 1556 $cm^{-1}$ for the sodium ionomer and 1622 and 1550 $cm^{-1}$ for the zinc ionomer. Normalized experimental data were fit using the Fickian solution for sorption/desorption of a small molecule (in this case ions) in a membrane:[17,18]

$$\frac{A_t - A_0}{A_\infty - A_0} = 1 - \frac{8}{\pi\lambda}\sum_{n=0}^{\infty}\frac{(-1)^n}{2n+1}\frac{1}{\frac{2}{\lambda} + \frac{(2n+1)^2\pi^2\lambda}{8L^2}\exp\left\{\frac{-D(2n+1)^2\pi^2 t}{4L^2}\right\}} \quad (2)$$

where $L$ is the membrane thickness and the other parameters are as previously defined. Experimental temperatures ranged from the semicrystalline state at 70 °C to well into the melt at 150 °C.

For measurements of the chain center of mass diffusion, the dissolution of a copolymer of 5.4 mol % methacrylic acid into a copolymer of 3.5 mol % methacrylic acid was tracked. Quantification was provided by integrating the area of the acid carbonyl peaks at 1749 and 1704 $cm^{-1}$, which correspond to acid monomer and dimer, respectively.[19] Normalized experimental data were fit using a Fickian solution for polymer mutual diffusion across an interface.[15]

$$\frac{A_t - A_0}{A_\infty - A_0} = 1 - \left(\frac{2}{\pi}\sum_{n=1}^{\infty}\frac{\sin\left(n\pi\frac{b}{a}\right)}{n} \exp\left(-n^2\pi^2\frac{Dt}{a^2}\right)\left[\frac{1 + (-1)^{n+1}\exp\left(\frac{-2a}{\lambda}\right)}{1 + \left(\frac{n\pi\lambda}{2a}\right)^2}\right] \Bigg/ \left(\left[1 - \exp\left(\frac{-2b}{\lambda}\right)\right] - \frac{b}{a}\left[1 - \exp\left(\frac{-2a}{\lambda}\right)\right]\right)\right) \quad (3)$$

Experimental temperatures ranged from 150 to 250 °C.

To begin an experiment, the diffusion couple is produced by placing the matrix film in contact with the ATR crystal coated with the penetrant thin film. A sheet of silicone rubber was used on the back of the thicker matrix film to ensure uniform mechanical contact in the polymer bilayer. This assembly was then mounted in a stainless steel cell which is equipped with resistive heating elements and a temperature controller. Once the assembly is aligned within an FTIR spectrometer, the spectrometer chamber is sealed and purged until the carboxylate bands shift to the absorption frequencies

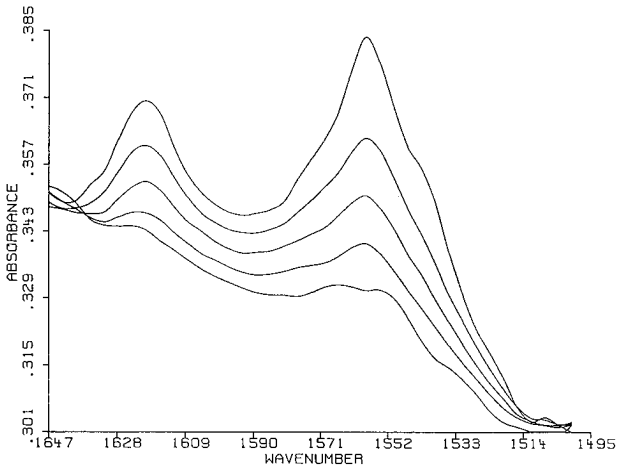


**Figure 1.** Infrared spectra showing the decreasing intensities of the asymmetric carboxylic salt absorptions with increasing time. These data are from a run utilizing a zinc ionomer in contact with an acid copolymer. The experimental times, proceeding from the top, are 0, 21.9, 66.4, 258.1, and 406.0 min.

**Table 2. Peak Positions and Half-Widths of Acid Group Absorptions**

| material | monomer acid peak ($cm^{-1}$) | "dimer acid" peak ($cm^{-1}$) | "dimer acid" fwhm ($cm^{-1}$) |
|---|---|---|---|
| E/MAA 1 | 1749 | 1704 | 16 |
| zinc ionomer | 1749 | 1698 | 27 |
| sodium ionomer | 1749 | 1693 | 37 |

characteristic of dry ionomer. Experiments commence by rapidly heating the cell from room temperature to the experimental temperature. The heating time was approximately 20 s for the largest interval between room temperature and the highest temperature used in this study (150 °C). Spectral acquisition proceeds automatically and is controlled by a macro programmed into the spectrometer. Typical raw data, in this case for the diffusion of the zinc ionomer, are illustrated as Figure 1.

Since we were also interested in the influence of water on ionic transport, several experiments were conducted on water-saturated films. These were prepared by first drying melt-pressed films of the sodium ionomer in a vacuum oven at 50 °C overnight and then soaking the films in a container of heavy water ($D_2O$) for at least 2 weeks prior to experimentation. This time frame is adequate to achieve complete saturation of the matrix.[20] When the bilayer films are assembled, a small amount of heavy water is placed in the bottom of the cell to maintain saturation.

**Infrared Measurements of Association.** Concurrent with this study, we utilized the vibrational spectra to obtain information on ionic and acid association as a function of temperature. In these instances, single-component films were contacted with the ATR element and spectra obtained in incremental heating and cooling cycles from 5 to 225 °C. As outlined by numerous authors,[19,21] the evaluation of the acid monomer and dimer concentration gives the value of the dimerization equilibrium constant, and the temperature dependence of these provides the enthalpy and entropy of dimerization through the van't Hoff relation:

$$\ln K = -\frac{\Delta H}{RT} + \frac{\Delta S}{R} \qquad (4)$$

We would like to highlight a complication to this analysis. Both the location of the carboxylic acid "dimer" peak and the peak shape (which we characterize by the full width at one-half of the peak maximum) clearly change upon neutralization as presented in Table 2. This shift to lower energy in the ionomers indicates that some fraction of these "dimer" acids participate in association with the metal ions. Furthermore, the large (ca. 2×) increase in peak width indicates that the

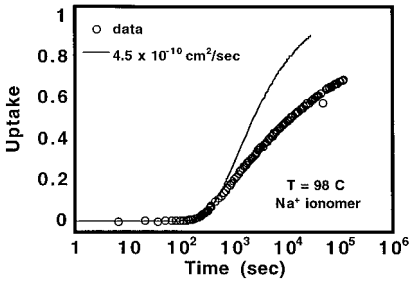


**Figure 2.** Normalized uptake data for the diffusion of sodium ions *into* the detection volume of the ATR experiment. The data undershoot the model prediction, indicating that the rate of diffusion slows as the concentration of ions in the detection volume increases.

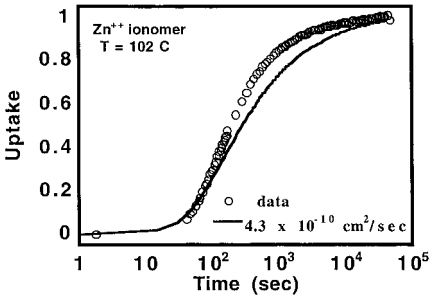


**Figure 3.** Normalized uptake data for the diffusion of zinc ions *out* of the detection volume of the ATR experiment. The data overshoot the model prediction, indicating that diffusion speeds up as the zinc concentration becomes more dilute.

number of microchemical environments of these "dimer" species increases dramatically upon neutralization. It is therefore likely that only a fraction of the energies underlying this peak can be properly assigned to true dimer acids. Although previous investigations have noted a shift in equilibrium toward dimerization with increasing neutralization,[19,22] this complication with the actual peak assignment does not appear to have been previously noted.

The carboxylate stretching region is also sensitive to changes in the environment of the ionic species.[19,21–23] Spectra from the diffusion experiments were examined to determine if discernible changes in the ionic environment occurred in these experiments. No discernible change was detected for either metal system.

## Results

**Diffusion.** The model of a single diffusion coefficient was generally found to provide an inadequate fit of the data across the course of an experiment. We observed that the transport process generally appeared to slow, with the data undershooting the model predictions in cases where the ions were penetrating into the detection volume of the experiment (Figure 2). Transport also appeared to accelerate in cases where ionic transport was out of the detection volume of the experiment (data overshoot (Figure 3)). These results indicate that ionic transport is sensitive to the local ionic concentration. We therefore emphasize that the ionic diffusion coefficients that we report are *initial* diffusion coefficients, i.e., those obtained from the earliest time data where the concentration difference is greatest.

For presentation, the observed diffusion coefficients were first normalized by dividing by the amorphous phase volume fraction. The temperature dependence of the diffusion coefficients is illustrated in Figure 4 and listed in Table 3. It is clear that the mobility of the ions in these materials falls into at least two distinct regimes characterized by markedly different activation energies, 12 kcal/mol above $T_m$ and 39 kcal/mol below $T_m$. Most

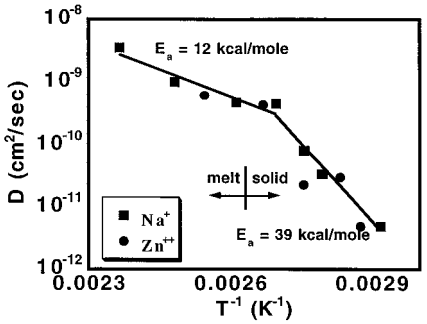


**Figure 4.** Activation plot for the initial diffusion coefficients of sodium and zinc ions in ionomer/acid copolymer bilayers. Note the break in the behavior at the melting temperature of the resin.

**Table 3**

| temp (°C) | $D \times 10^{12}$ (cm²/s) | $\Phi_{amorph}$ |
|---|---|---|
| Diffusion of Ions in Dry Sodium Ionomer[a] | | |
| 70 | 6 ± 1 | 0.82 |
| 85 | 38 ± 2 | 0.86 |
| 90 | 90 ± 10 | 0.89 |
| 98 | 460 ± 30 | 0.97 |
| 110 | 470 ± 40 | 1 |
| 130 | 900 ± 10 | 1 |
| 150 | 3500 ± 1000 | 1 |
| Diffusion of Ions in $D_2O$-Saturated Sodium Ionomer[a] | | |
| 80 | 95 ± 10 | 0.84 |
| 90 | 200 ± 20 | 0.89 |
| Diffusion of Ions in Dry Zinc Ionomer[a] | | |
| 75 | 3.5 ± 0.1 | 0.83 |
| 80 | 36 ± 1 | 0.84 |
| 90 | 26 ± 4 | 0.89 |
| 102 | 430 ± 20 | 1 |
| 120 | 600 ± 200 | 1 |

[a] Coefficients have been normalized by $\Phi_{amorph}$.

**Table 4. Initial Diffusion Coefficients for E/MAA 1 into E/MAA 2[a]**

| temp (°C) | $D_{init} \times 10^{12}$ (cm²/s) |
|---|---|
| 150 | 5 |
| 200 | 35 |
| 246 | 200 |

[a] These data are only valid as upper limits (see text).

interestingly, this intersection of the two regimes occurs at a temperature of 98 °C, which is near the 107 °C melting point of the resin. Although we would anticipate a difference in mobility of the zinc and sodium ions due to a difference in both the mass and valency of these ions, within the precision of our measurements, we are unable to discern this. Our experiments using $D_2O$-saturated films generally gave diffusion coefficients higher by a factor of 2 than those observed for the dry materials.

Measurements of chain center of mass diffusion range are provided in Table 4. As the temperature of the measurement decreased, our ability to establish good fits to the data diminished. This was not surprising given the very high polydispersity (ca. 8) and the presence of long chain branching in the materials. Consequently, these particular results are only useful in establishing *upper limits* for the center of mass diffusion process; we present them for the sole purpose of contrasting the magnitude of the ionic diffusion process to the polymer chain diffusion process. This disparity in rate also made it necessary to obtain these measurements at substantially higher temperatures than the ionic measurements to compensate for the much more sluggish transport process. At 150 °C, for example, the difference in diffusion coefficients between the sodium ions and the chain center of mass is 3 orders of magnitude. We note that these chain diffusion coefficients represent an upper limit as well, since the dominant portion of the diffusion couple was a copolymer 8 times lower in melt viscosity than the parent copolymer of the ionomers studied. Arrhenius analysis gives an activation energy for diffusion of 17 kcal/mol.

## Discussion

**Ionic Diffusion.** These observations provide significant insight into the details of ionic transport in these materials. First, the fact that the transport behavior shows a break near the melting temperature of the matrix indicates either that ionic transport is hindered by the presence of crystallites within the matrix or that ionic mobility depends to some extent on the mobility of chain backbones. Given the very low degrees of crystallinity in the temperature range investigated (ca. 0−0.1 volume fraction), it is unlikely that percolation or tortuosity phenomena affect ionic transport. The observation that the activation energy for ionic diffusion is significantly greater below the melting temperature of the resin is also indicative of a process significantly hindered by the anchoring of chains. It is therefore apparent that ionic mobility in these systems depends intimately on the mobility of the chain backbone.

It is also notable that the ionic diffusion coefficients are several orders of magnitude higher than center of mass coefficients characteristic of the polymer melts. Below the ionomer melting temperature this disparity would be further magnified as the only extant mechanism for chain center of mass motion necessitates the very slow slippage of backbones through crystals.[24] Given the very sluggish nature of chain center of mass motion, it is apparent that ions must be exchanged from chain to chain within the melt. Vyprachticky et al. in a study of ionic diffusion through ionomers of methacrylates and acrylates concluded that transport was dominated by the mobility of free ions.[13] Perhaps coincidentally, the diffusion coefficients measured by these investigators are of the same order of magnitude as those measured in this work. In contrast, we believe that it is highly unlikely that an appreciable number of free ions exist within the low dielectric constant hydrocarbon medium we describe and so instead postulate that transport must involve the motion of an ion *pair*. In addition, our observations (via vibrational spectra) that the ionic environment is relatively unchanged suggest that the *structure* of the multiplets remains unchanged while their concentration diminishes.

We are thus challenged with describing a mechanism for high mobility of ion pairs in a case with very restricted backbone mobility. In addition, our model should also explain the increase in mobility with decreasing neutralization and saturation with water and the observed weak dependence on ion valency. One way that these observations may be accommodated is a mechanism by which ionic transport occurs along chain backbones. In this picture, local conformational changes bring neighboring acid groups together, allowing intra- and intermolecular exchange of metal ions and protons in a transport process that occurs along the backbone of chains. In this way, ions hop between acid sites and are transported along the contour of the polymer network.

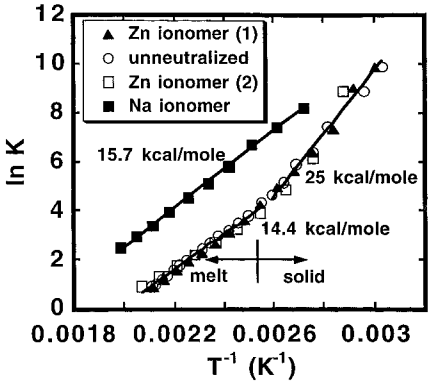


**Figure 5.** van't Hoff plot of the equilibrium constants for dimerization of acid groups from four separate experiments. Note the break in the behavior at the resin melting temperature, with two distinct enthalpies of dimerization above and below this point. Increasing neutralization results in a shift toward dimerization, as illustrated by the behavior of the sodium ionomer. Interestingly, no break was observed in the plot for the sodium ionomer.

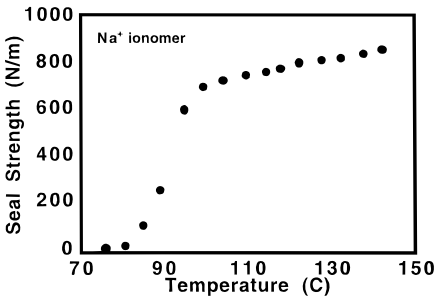


**Figure 6.** Seal strength versus sealing temperature for sodium ionomer film.

The presence of even a small amount of crystallinity reduces ionic diffusion by restricting the freedom of local backbone motion, anchoring the chain and allowing only limited wandering of the liquid fraction. Crystallinity might also decrease ionic diffusion rates by preventing the formation of free acid. This latter effect is seen in the acid dimerization data for the zinc ionomer, which we present as Figure 5. As with the transport data, there is a clear break in the curve at the resin melting temperature, with two regimes characterized by different enthalpies of association. Similar behavior has been noted at the glass transition of an amorphous ionomer.[22] Crystallinity can be seen as an excess force which drives the equilibrium to dimerization and so would tend to diminish the concentration of free acid necessary to "attack" an ion pair and transfer the metal.

The decrease in the rate of ionic diffusion with increasing neutralization (as observed in the deviations from single diffusion coefficient behavior) can be explained in a similar fashion. As neutralization increases, the backbone mobility and the concentration of free acid diminish, both of which will decrease the rate at which ions are exchanged along the network contour.

**Seal Strength.** A typical "heat seal curve" is presented as Figure 6. In commercial applications, one of the most critical aspects of the heat seal behavior is the "seal initiation temperature", or the temperature at which significant interfacial strength begins to be built. Figure 6 indicates that this corresponds to a temperature of ca. 95 °C. A more direct correlation with molecular structure, however, is found by replotting these data semilogarithmically against the fractional

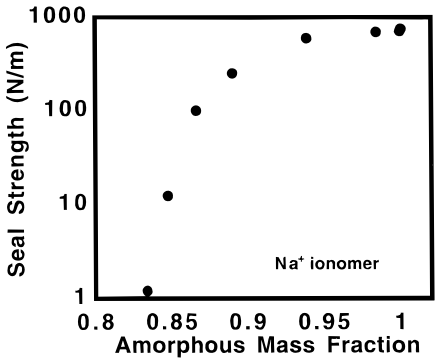


**Figure 7.** Dependence of the seal strength on resin melting for the sodium ionomer film.

**Table 5. Interpenetration Distances for Sodium Ions**

| temp (°C) | $x$ (Å) |
|---|---|
| 70 | 350 |
| 90 | 1300 |
| 110 | 3000 |
| 130 | 4200 |
| 150 | 8400 |

amorphous content as presented in Figure 7. This shows that interfacial strength is determined primarily by those molecular processes which occur as the last crystallinity is erased from the material.

Most theories of strength development describe two dominant processes, namely the formation of interfacial contact on a molecular scale and the subsequent interdiffusion of the two polymer phases. Our challenge is to determine the relative importance of these two components. The observation that seal strength is independent of contact pressure indicates that variations from the former mechanism may be discounted. Under these conditions, the formation of contact area is not the strength-determining step.

It thus appears that interdiffusion is the key to building strong interfaces. The question now arises whether this strength can be built simply by the rapid rearrangement of the ionic network or instead requires the much more sluggish interdiffusion of polymer chains. Table 5 provides the estimated diffusion distances $(2Dt)^{1/2}$ for these ions over the 1 s sealing time used in this study. It is immediately apparent that even at the lowest temperatures these distances greatly exceed any characteristic dimension of a polymer chain or the ionic network. Since it is apparent that resin melting is a prerequisite for high strength, we can conclude that the interchange of ionic groups is insufficient by itself for building strong interfaces.

If we now estimate the extent of polymer backbone interdiffusion, a much more plausible dependence emerges. Using the diffusion coefficients from the acid copolymer backbones, we estimate that the extent of interpenetration is roughly 80 Å at 100 °C. This dimension is a far more characteristic of an interface that has not yet been completely erased. We note that even this length represents an upper limit, since it may be assumed that the extrapolation of melt diffusion coefficients into even the last stages of melting is at best haphazard. Our picture of interfacial strength development then becomes identical to that of a host of other thermoplastics, in which melting liberates chain diffusion, which enables welding to proceed.

## Conclusions

The diffusion of ions in ionomers of poly(ethylene-*co*-methacrylic acid) shows a striking dependence on the

state of the material. A break in the diffusion behavior at the resin melting temperature is taken to be indicative that chain backbone motions are intimately involved in the mechanism of ionic transport. These results suggest that in these systems ionic transport does not occur by dissociated ions but instead by a process in which the metal cation is exchanged with a proton from a neighboring acid group and is thereby transported along the contour of the polymer network.

Interfacial strength development for these materials is shown to be intimately dependent on the melting behavior of the bulk resin. Ionic diffusion appears to be far too rapid to account for the observed dependence of seal strength on temperature. Instead, melting appears to liberate chain interdiffusion, enabling welding to proceed in a manner common to many other thermoplastics.

**Acknowledgment.** We are indebted to J. R. de Garavilla of the Dupont Sabine River Laboratory for providing the materials and the seal strength data. Diffusion experiments were performed with the able assistance of B. C. Cox, and thermal analysis was provided by W. G. Kampert.

## References and Notes

(1) Dodin, M. G. *J. Adhes.* **1981**, *12*, 99.
(2) Jud, K.; Kausch, H. H.; Williams, J. G. *J. Mater. Sci.* **1981**, *16*, 204.
(3) Brown, H. R.; Yang, A. C. M.; Russell, T. P.; Volksen, W.; Kramer, E. J. *Polymer* **1988**, *29*, 1807.
(4) Lustig, S. R.; Van Alsten, J. G.; Hsiao, B. *Macromolecules* **1993**, *26*, 3885.
(5) Van Alsten, J. G.; Lustig, S. R.; Hsiao, B. *Macromolecules* **1995**, *28*, 3672.
(6) Van Alsten, J. G.; Sauer, B. B.; Gochanour, C. R.; Faron, K. T. *Macromolecules* **1995**, *28*, 7019.
(7) Meka, P.; Stehling, F. C. *J. Appl. Polym. Sci.* **1994**, *51*, 89.
(8) Stehling, F. C.; Meka, P. *J. Appl. Polym. Sci.* **1994**, *51*, 105.
(9) Eisenberg, A.; King, M. *Ion Containing Polymers*; Academic Press: New York, 1977.
(10) Hird, B.; Eisenberg, A. *Macromolecules* **1992**, *25*, 6466.
(11) Tant, M. R.; Wilkes, G. L. *J. Macromol. Sci., Rev. Macromol. Chem. Phys.* **1988**, *C28*, 1.
(12) Gronowski, A. A.; Jiang, M.; Yeager, H. L.; Wu, G.; Eisenberg, A. *J. Membr. Sci.* **1993**, *82*, 83.
(13) Vyprachticky, D.; Morawetz, H.; Fainzilberg, V. *Macromolecules* **1993**, *26*, 339.
(14) Tadano, K.; Hirasawa, E.; Yamamoto, H.; Yano, S. *Macromolecules* **1989**, *22*, 226.
(15) Van Alsten, J. G.; Lustig, S. R. *Macromolecules* **1992**, *25*, 5069.
(16) Harrick, N. J. *Internal Reflection Spectroscopy*; John Wiley & Sons: New York, 1967; p 63.
(17) Crank, J. *The Mathematics of Diffusion*; Oxford University Press: Oxford, 1956; p 44.
(18) Van Alsten, J. G.; Coburn, J. C. *Macromolecules* **1994**, *27*, 3746.
(19) Van Alsten, J. G., manuscript in preparation.
(20) Earnest, T. R.; MacKnight, W. J. *Macromolecules* **1980**, *13*, 844.
(21) MacKnight, W. J.; McKenna, L. W.; Read, B. E.; Stein, R. S. *J. Phys. Chem.* **1968**, *72*, 1122.
(22) Ogura, K.; Sobue, H.; Nakamura, S. *J. Polym. Sci., Polym. Phys. Ed.* **1973**, *11*, 2079.
(23) Painter, P. C.; Brozoski, B. A.; Coleman, M. M. *J. Polym. Sci., Polym. Phys. Ed.* **1982**, *20*, 1069.
(24) Arridge, R. G.; Parham, P. J. *Polymer* **1978**, *19*, 603.

MA950431F